

# Three-Loop Radiative-Recoil Corrections to Hyperfine Splitting: Diagrams with Polarization Loops

Michael I. Eides\*

*Department of Physics and Astronomy,  
University of Kentucky, Lexington, KY 40506, USA,*

Valery A. Shelyuto†

*D. I. Mendeleev Institute of Metrology, St.Petersburg 190005, Russia*

(Dated: July 7, 2009)

## Abstract

We consider three-loop radiative-recoil corrections to hyperfine splitting in muonium generated by the diagrams with electron and muon vacuum polarizations. We calculate single-logarithmic and nonlogarithmic contributions of order  $\alpha^3(m/M)E_F$  generated by gauge invariant sets of diagrams with electron and muon polarization insertions in the electron and muon factors. Combining the new contributions with our older results we present complete result for all three-loop radiative-recoil corrections generated by the diagrams with electron and muon polarization loops.

arXiv:0907.1923v1 [hep-ph] 10 Jul 2009

The radiative-recoil corrections of order  $\alpha^3(m/M)E_F$  to hyperfine splitting are enhanced by large logarithm of the muon-electron mass ratio  $M/m$  [1]. The leading logarithm cubed and logarithm squared contributions are generated by the graphs with the electron closed loops in Figs. 1-4 (and by the diagrams with the crossed exchanged photon lines), and were calculated long time ago [1, 2]

$$\Delta E = \left( -\frac{4}{3} \ln^3 \frac{M}{m} + \frac{4}{3} \ln^2 \frac{M}{m} \right) \frac{\alpha^3 m}{\pi^3 M} E_F. \quad (1)$$

The Fermi energy  $E_F$  here does not include the muon anomalous magnetic moment  $a_\mu$  that does not factorize in the case of recoil corrections, and should be considered on the same grounds as other corrections to hyperfine splitting.

Single-logarithmic and nonlogarithmic terms of order  $\alpha^3(m/M)\tilde{E}_F$  are generated by all diagrams in Figs. 1-4, by the respective graphs with the muon loops, by the graphs with polarization and radiative photon insertions in the muon line, and also by the three-loop graphs with radiative photons in the electron and/or muon lines but without polarization loops. Below we calculate three-loop single-logarithmic and nonlogarithmic radiative-recoil corrections generated by the diagrams in Figs. 5, 6 both with the electron and muon loops. We also combine these corrections with our earlier results and present complete results for all radiative-recoil corrections generated by the diagrams with electron and muon polarizations.

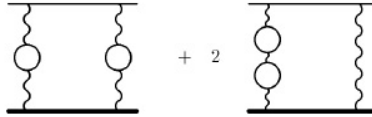


FIG. 1: Graphs with two one-loop polarization insertions

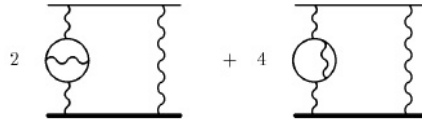


FIG. 2: Graphs with two-loop polarization insertions

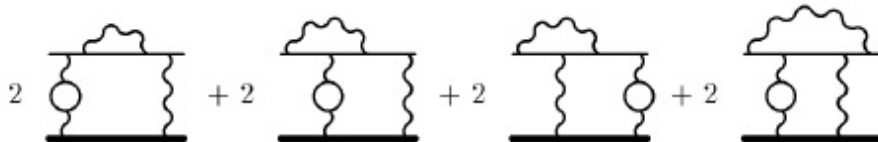


FIG. 3: Graphs with radiative photon insertions

It is convenient to consider the three-loop diagrams in Figs. 5, 6 as radiative corrections to the skeleton diagrams with two-photon exchanges in Fig. 7. Naive momentum integral for the skeleton diagrams contribution to HFS is linearly divergent at low integration momenta of order  $m\alpha$ . This linear divergence corresponds to the classic nonrecoil Fermi contribution

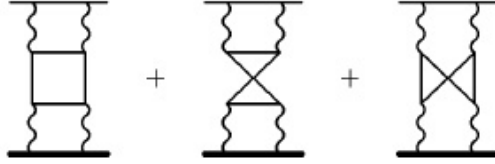


FIG. 4: Graphs with light by light scattering insertions

to HFS and should be subtracted in calculation of recoil contribution generated by the diagrams in Fig. 7. After subtraction the momentum integral for these diagrams becomes logarithmic in the wide integration region  $m \leq k \leq M$  and generates the leading recoil correction to HFS. The integration momenta for the leading recoil correction are much larger than the atomic scale virtuality  $m\alpha$  of the external line, and we can omit this virtuality and calculate matrix elements in the scattering regime between the free electron and muon spinors. We can consider the momentum integrand in the skeleton case as a product of the skeleton electron (muon) factor  $L_{\mu\nu}(k)$  and the remaining part of the diagram. The skeleton factor  $L_{\mu\nu}(k)$  is the skeleton Compton scattering amplitude for virtual photons. Contributions to HFS generated by the diagrams in Figs. 5, 6 are described by the integrals similar to the skeleton integrals for the diagrams in Fig. 7. The only difference is that for the diagrams in Figs. 5, 6 we need to include in the integral radiatively corrected virtual Compton scattering amplitude instead of the skeleton one. One can prove a generalized low energy theorem for the virtual Compton scattering amplitude with subtracted anomalous magnetic moment contribution (see more on this subtraction below) [3, 4]. According to this theorem the electron (muon) factor  $L_{\mu\nu}(k)$  is suppressed in comparison with the respective skeleton factor by an additional factor  $k^2/m^2$  ( $k^2/M^2$ ). Due to this additional suppression the integrals for contributions to HFS generated by the diagrams in Figs. 5, 6 are infrared finite and the integration region with momenta less than the electron mass are additionally suppressed. Therefore, as in the case of the skeleton recoil corrections in Fig. 7, we can omit the atomic scale external virtualities of order  $m\alpha$ , and calculate matrix elements in the scattering regime between the free electron and muon spinors. Matrix elements turn into contributions to HFS after multiplication by the Coulomb-Schrödinger bound state wave function at the origin squared, and calculation of differences between spin one and spin zero states. We use the Feynman gauge to obtain matrix elements of the gauge invariant sets of diagrams in Figs. 5, 6. Each of the diagrams in Figs. 5, 6 contains polarization operator insertion in one of the radiative photon lines. We account for these insertions using the massive photon propagator for radiative photons (but not for exchanged photons) with the photon mass squared  $\lambda^2 = 4m^2/(1 - v^2)$  or  $\lambda^2 = 4M^2/(1 - v^2)$  for the the electron and muon polarization loops, respectively. Insertion of the polarization operator in the radiative photon line is accompanied by an additional integration over velocity  $v$  with the weight  $\int_0^1 dv v^2 (1 - v^2/3)/(1 - v^2)$ .

The diagrams in Fig. 5 with the electron polarization loops generate nonrecoil and logarithm squared, single-logarithmic, and nonlogarithmic radiative-recoil contributions to HFS. The electron anomalous magnetic moment terms are subtracted from the vertex corrections in these diagrams (as well as the muon anomalous magnetic moment terms are subtracted from the vertex corrections in the diagrams in Fig. 6 below). Technically the gauge invariant anomalous magnetic moment is the hardest entry in the expression for the vertex at small transferred momenta, and this prompts its separation. It turns out that the anomalous

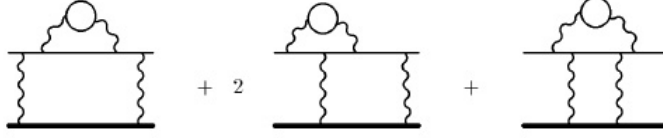


FIG. 5: Graphs with polarization insertions in the electron factor

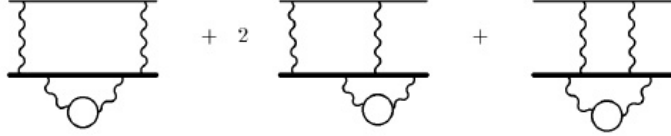


FIG. 6: Graphs with polarization insertions in the muon factor

magnetic moment in these diagrams does not generate radiative-recoil corrections (see, e.g., [4, 5]). As we mentioned above the radiatively corrected electron factor  $L_{\mu\nu}$  provides an additional suppression factor  $k^2/m^2$  in the skeleton integral over the exchanged momenta. This suppression is effective only for momenta smaller than the electron mass, and the wide integration region between the electron and muon masses  $m \leq k \leq M$  remains logarithmic. We calculated the nonrecoil contribution numerically, the logarithm squared and single-logarithmic terms analytically, and the nonlogarithmic term numerically. The logarithm squared terms is already well known [2], and the single-logarithmic and nonlogarithmic contributions are as follows

$$\Delta E = \left[ \left( \pi^2 - \frac{53}{6} \right) \ln \frac{M}{m} + 7.0807 \right] \frac{\alpha^3 m}{\pi^3 M} E_F. \quad (2)$$

The electron factor with muon polarization insertions in the diagrams in Fig. 5 provides an additional suppression factor  $k^2/M^2$ , and lifts characteristic integration momenta to the scale of the muon mass. Then these diagrams with the muon polarization loops do not generate nonrecoil contributions to HFS, all of which originate from the region of nonrelativistic muon momenta. The suppression factor also ruins the logarithmic nature of integration in the region  $m \leq k \leq M$ , and the leading recoil correction generated by the diagrams in Fig. 5 with the muon polarization insertions becomes is a pure number. We calculated it numerically

$$\Delta E = -1.3042 \frac{\alpha^3 m}{\pi^3 M} E_F. \quad (3)$$

Consider now diagrams in Fig. 6 with radiative corrections in the muon line. The ra-



FIG. 7: Diagrams with two-photon exchanges

diatively corrected muon factor provides an additional suppression factor  $k^2/M^2$  in the exchanged momentum integral for radiative-recoil corrections in comparison with the respective skeleton integral for the diagrams in Fig. 7. Hence, these diagrams do not generate nonrecoil contributions to HFS, and the integral over the exchanged momenta is nonlogarithmic. There is, however, another source of large logarithms in the case of electron polarization insertions in Fig. 6. All characteristic momenta in these diagrams are of order of the muon mass  $M$ . Then the electron polarization insertions in the diagrams in Fig. 6 enter in the asymptotic regime, and the leading contribution to HFS generated by the diagrams with the electron polarization insertions in Fig. 6 is just the product of the leading asymptotic term in the high momentum expansion of the electron polarization operator and the radiative-recoil correction to HFS generated by the one-loop muon factor without polarization insertions. In other words the leading logarithmic contribution to HFS generated by the diagrams in Fig. 6 is obtained from the respective nonlogarithmic contribution of the diagrams without polarization insertions by substitution of the running coupling constant  $\alpha(M)$  for radiative photons. We calculated also the nonlogarithmic contribution and obtained

$$\Delta E = \left[ \left( 3\zeta(3) - 2\pi^2 \ln 2 + \frac{13}{4} \right) \ln \frac{M}{m} + 12.227(2) \right] \frac{\alpha^3 m}{\pi^3 M} E_F. \quad (4)$$

The muon factor with muon polarization loops in the diagrams in Fig. 6 again provides the suppression factor  $k^2/M^2$ , but no enhancements. As a result these diagrams generate only nonlogarithmic radiative-recoil corrections. After numerical calculations we obtained

$$\Delta E = -0.931 \frac{\alpha^3 m}{\pi^3 M} E_F. \quad (5)$$

Other single-logarithmic and nonlogarithmic three-loop radiative-recoil corrections generated by the diagrams with electron and muon polarization insertions were obtained earlier, and we collect respective results below. Single-logarithmic and nonlogarithmic radiative-recoil corrections generated by the diagrams with two electron or two muon loops in Fig. 1 are [6]

$$\Delta E = \left[ - \left( \frac{2\pi^2}{3} + \frac{25}{9} \right) \ln \frac{M}{m} - \frac{4\pi^2}{9} - \frac{535}{108} \right] \frac{\alpha^3 m}{\pi^3 M} E_F. \quad (6)$$

The diagrams with one electron and one muon loop in Fig. 8 produce only single-logarithmic and nonlogarithmic contributions to HFS [6]

$$\Delta E = \left[ \left( \frac{2\pi^2}{3} - \frac{20}{9} \right) \ln \frac{M}{m} + \frac{\pi^2}{3} - \frac{53}{9} \right] \frac{\alpha^3 m}{\pi^3 M} E_F. \quad (7)$$

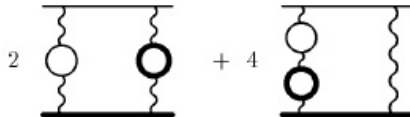


FIG. 8: Graphs with both the electron and muon loops

The single-logarithmic and nonlogarithmic radiative-recoil contributions to HFS generated by the diagrams in Fig. 2 with two-loop electron or two-loop muon polarization insertions were calculated analytically [6]

$$\Delta E = \left[ -\left(6\zeta(3) + \frac{13}{4}\right) \ln \frac{M}{m} - \frac{97}{8}\zeta(3) - 16\text{Li}_4\left(\frac{1}{2}\right) + \frac{2\pi^2}{3} \ln^2 2 - \frac{2}{3} \ln^4 2 + \frac{5\pi^4}{36} - \frac{\pi^2}{4} + \frac{7}{16} \right] \frac{\alpha^3 m}{\pi^3 M} E_F. \quad (8)$$

The single-logarithmic and nonlogarithmic radiative-recoil contributions generated by the diagrams with electron or muon polarization insertions in the exchanged photons in Fig. 3 have the form [7]

$$\Delta E = \left( \frac{10}{3} \ln \frac{M}{m} + 8.6945 \right) \frac{\alpha^3 m}{\pi^3 M} E_F. \quad (9)$$

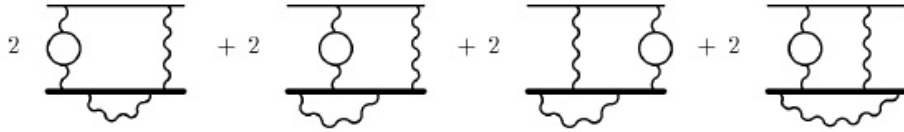


FIG. 9: Muon line and electron vacuum polarization

The diagrams in Fig. 9 with the electron or muon polarization insertions in the exchanged photons generate only single-logarithmic and nonlogarithmic radiative-recoil contributions to HFS [7]

$$\Delta E = \left[ \left( 6\zeta(3) - 4\pi^2 \ln 2 + \frac{5}{2} \right) \ln \frac{M}{m} + 23.8527 \right] \frac{\alpha^3 m}{\pi^3 M} E_F.$$

Combining all three-loop single-logarithmic and nonlogarithmic radiative-recoil corrections to hyperfine splitting due to electron and muon polarization loops in Eq. (2) - Eq. (10) we obtain

$$\Delta E_{tot} = \left[ \left( 3\zeta(3) - 6\pi^2 \ln 2 + \pi^2 - 8 \right) \ln \frac{M}{m} + 27.666 (2) \right] \frac{\alpha^3 m}{\pi^3 M} E_F.$$

For completeness let us mention that the three-loop radiative-recoil correction generated by the diagrams with one-loop fermion factors (and without polarization loops) in Fig. 10 is also known [8]

$$\Delta E = \left( -\frac{15}{8}\zeta(3) + \frac{15\pi^2}{4} \ln 2 + \frac{27\pi^2}{16} - \frac{147}{32} \right) \frac{\alpha^3 m}{\pi^3 M} E_F. \quad (10)$$

The only still unknown single-logarithmic and nonlogarithmic three-loop radiative-recoil corrections are generated by the gauge invariant sets of diagrams with two-loop fermion factors without polarization insertions, and the diagrams with light-by-light insertions in the exchanged photons. Calculation of these corrections is a task for the future.

Total result for all known three-loop single-logarithmic and nonlogarithmic radiative-recoil corrections to hyperfine splitting generated by the diagrams with electron, muon, and photon lines we obtain adding contributions in Eq. (10) and Eq. (10)

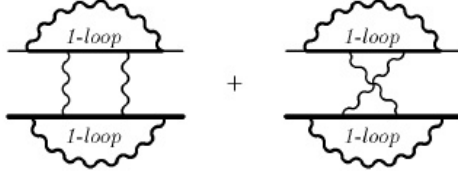


FIG. 10: Diagrams with two fermion factors

$$\Delta E_{tot} = \left[ \left( 3\zeta(3) - 6\pi^2 \ln 2 + \pi^2 - 8 \right) \ln \frac{M}{m} + 63.127 (2) \right] \frac{\alpha^3 m}{\pi^3 M} E_F.$$

Numerically this contribution to HFS in muonium is

$$\Delta E_{tot} = -0.0347 \text{ kHz.} \quad (11)$$

Currently the theoretical accuracy of hyperfine splitting in muonium is about 70 Hz. A realistic goal is to reduce this uncertainty below 10 Hz (see a more detailed discussion in [7, 9, 10]). The muon and electron polarization operator contributions and other corrections collected in Eq. (11), together with the results of comparable magnitude in [11, 12, 13, 14, 15, 16] constitute a next step toward achievement of this goal. Phenomenologically, the improved accuracy of the theory of hyperfine splitting would lead to a reduction of the uncertainty of the value of the electron-muon mass ratio derived from the experimental data [17] on hyperfine splitting (see, e.g., reviews in [9, 10, 18]).

This work was supported by the NSF grant PHY-0757928.

---

\* Also at Petersburg Nuclear Physics Institute, Gatchina, St.Petersburg 188300, Russia; Electronic address: eides@pa.uky.edu, eides@thd.pnpi.spb.ru

† Electronic address: shelyuto@vniim.ru

- [1] M. I. Eides and V. A. Shelyuto, Phys. Lett. B **146**, 241 (1984).
- [2] M. I. Eides, S. G. Karshenboim, and V. A. Shelyuto, Phys. Lett. B **216**, 405 (1989); Yad. Fiz. **49**, 493 (1989) [Sov. J. Nucl. Phys. **49**, 309 (1989)].
- [3] S. G. Karshenboim, V. A. Shelyuto, and M. I. Eides, Yad. Fiz. **47**, 454 (1988) [Sov. J. Nucl. Phys. **47**, 287 (1988)].
- [4] M. I. Eides, S. G. Karshenboim, and V. A. Shelyuto, Ann. Phys. (NY) **205**, 291 (1991).
- [5] S. G. Karshenboim, V. A. Shelyuto, and M. I. Eides, Zh. Eksp. Teor. Fiz. **94**, 42 (1988) [Sov. Phys.-JETP **67**, 671 (1988)].
- [6] M. I. Eides, H. Grotch, and V. A. Shelyuto, Phys. Rev. D **65**, 013003 (2001).
- [7] M. I. Eides, H. Grotch, and V. A. Shelyuto, Phys. Rev. D **67**, 113003 (2003).
- [8] M. I. Eides, H. Grotch, and V. A. Shelyuto, Phys. Rev. D **70**, 073005 (2004).
- [9] M. I. Eides, H. Grotch, and V. A. Shelyuto, Phys. Rep. **342**, 63 (2001).
- [10] M. I. Eides, H. Grotch, and V. A. Shelyuto, *Theory of Light Hydrogenic Bound States*, (Springer, Berlin, Heidelberg, New York, 2007).
- [11] M. I. Eides, H. Grotch, and V. A. Shelyuto, Phys. Rev. D **58**, 013008 (1998).
- [12] K. Melnikov and A. Yelkhovsky, Phys. Rev. Lett. **86**, 1498 (2001).
- [13] R. J. Hill, Phys. Rev. Lett. **86**, 3280 (2001).

- [14] S. G. Karshenboim and V. A. Shelyuto, Phys.Lett. B **517**, 32 (2001).
- [15] A. Czarnecki, S. I. Eidelman, and S. G. Karshenboim, Phys. Rev. D **65**, 053004 (2002).
- [16] S. G. Karshenboim, V. A. Shelyuto, and A. I. Vainshtein, Phys. Rev. D **78**, 065036 (2008).
- [17] W. Liu, M. G. Boshier, S. Dhawan et al, Phys. Rev. Lett. **82**, 711 (1999).
- [18] P. J. Mohr and B. N. Taylor, Rev. Mod. Phys. **80**, 633 (2008).